

## Understanding molecular structure dependence of exciton diffusion in conjugated small molecules

Zi Li, Xu Zhang, Cristiano F. Woellner, and Gang Lu

Citation: [Applied Physics Letters](#) **104**, 143303 (2014); doi: 10.1063/1.4871303

View online: <http://dx.doi.org/10.1063/1.4871303>

View Table of Contents: <http://scitation.aip.org/content/aip/journal/apl/104/14?ver=pdfcov>

Published by the [AIP Publishing](#)

---

### Articles you may be interested in

[Exciton coherence lifetimes from electronic structure](#)

J. Chem. Phys. **136**, 104510 (2012); 10.1063/1.3689858

[Measurement of exciton diffusion lengths in optically thin organic films](#)

Appl. Phys. Lett. **99**, 243303 (2011); 10.1063/1.3668106

[Exciton diffusion and relaxation in methyl-substituted polyparaphenylene polymer films](#)

J. Chem. Phys. **127**, 144907 (2007); 10.1063/1.2790901

[Proton transfer in imidazole-based molecular crystals](#)

J. Chem. Phys. **124**, 204710 (2006); 10.1063/1.2202323

[Exciton migration dynamics in a dendritic molecule: Quantum master equation approach using ab initio molecular orbital configuration interaction method](#)

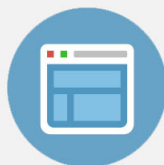
J. Chem. Phys. **120**, 2359 (2004); 10.1063/1.1636723

---



## Re-register for Table of Content Alerts

Create a profile.



Sign up today!



## Understanding molecular structure dependence of exciton diffusion in conjugated small molecules

Zi Li,<sup>1</sup> Xu Zhang,<sup>1</sup> Cristiano F. Woellner,<sup>2</sup> and Gang Lu<sup>1,a)</sup>

<sup>1</sup>Department of Physics and Astronomy, California State University, Northridge, California 91330-8268, USA

<sup>2</sup>Departamento de Física, Universidade Federal do Paraná, 81531-990 Curitiba-PR, Brazil

(Received 7 February 2014; accepted 2 April 2014; published online 8 April 2014)

First-principles simulations are carried out to understand molecular structure dependence of exciton diffusion in a series of small conjugated molecules arranged in a disordered, crystalline, and blend structure. Exciton diffusion length ( $L_D$ ), lifetime, and diffusivity in four diketopyrrolopyrrole derivatives are calculated and the results compare very well with experimental values. The correlation between exciton diffusion and molecular structure is examined in detail. In the disordered molecule structure, a longer backbone length leads to a shorter exciton lifetime and a higher exciton diffusivity, but it does not change  $L_D$  substantially. Removal of the end alkyl chains or the extra branch on the side alkyl chains reduces  $L_D$ . In the crystalline structure, exciton diffusion exhibits a strong anisotropy whose origin can be elucidated from the intermolecular transition density interaction point of view. In the blend structure,  $L_D$  increases with the crystalline ratios, which are estimated and consistent with the experimental results. © 2014 AIP Publishing LLC. [<http://dx.doi.org/10.1063/1.4871303>]

Exciton diffusion is crucial to the performance of organic photovoltaics (OPVs). The molecular excitons generated by light absorption have to migrate to the donor/acceptor interfaces within their lifetimes for charge separation.<sup>1</sup> Hence, exciton diffusion length ( $L_D$ ) is a key material parameter in designing OPVs. Although a number of experimental techniques<sup>2–13</sup> have been developed to measure  $L_D$  in both polymers and small molecules, they sometimes yielded different  $L_D$  values for the same material (e.g., P3HT).<sup>7,11–13</sup> More importantly, it is not always possible to establish connections between experimental measurements and their physical underpinnings. In particular, there is a lack of understanding on molecular structure dependence of exciton diffusion, e.g., the correlation between molecular structure (conjugation length, functional group, molecular rigidity, and crystallinity) and  $L_D$ . Gaining such understanding is essential to rational material design for highly efficient OPVs.

To address these challenges, Lin *et al.* have carried out systematic study on exciton diffusion in a series of conjugated small molecules using a variety of experimental techniques.<sup>14</sup> They found that reducing molecular size and bulkiness of solubilizing groups resulted in an enhancement of exciton diffusion coefficient and diffusion length. In addition, since the materials contained blends of crystalline and disordered domains, they attributed different diffusion coefficients to different crystalline/disorder ratios of the materials. In this paper, we expand on the experimental investigations and carry out first-principle simulations to determine exciton diffusion length, diffusivity, and lifetime in the same materials as examined in the experiments. The goal of this paper is to elucidate molecular underpinnings of exciton diffusion, validate both the simulation and experimental results and correlate the molecular structure with exciton diffusion properties. In addition, since experimental measurements of  $L_D$  are very time-consuming, the first-

principles simulations, once sufficiently validated, could offer an alternative to experiments for determining  $L_D$ .

Exciton diffusion in the disordered molecular domain is modeled by our recently developed first-principles method,<sup>15</sup> which includes a range-separated hybrid exchange-correlation functional<sup>16–18</sup> for determining exciton energies and many-body wave-functions, along with a non-adiabatic molecular dynamics<sup>19–21</sup> for evaluating exciton transition rates. Exciton diffusion in a crystalline structure is determined by a well-developed approach combining Förster model<sup>22–25</sup> with first-principles calculations of exciton coupling and reorganization energies. Exciton diffusion in a blend structure is simulated by considering exciton hopping rates from both the disordered and crystalline domains. The computational details can be found in the supplementary material.<sup>26</sup>

Four small diketopyrrolopyrrole (DPP) molecules are examined in this paper: 2,5-Dihexyl-3,6-bis[4-(5-hexylthiophene-2-yl)phenyl]-pyrrolo[3,4-c]-pyrrole-1,4-dione, 2,5-Dihexyl-3,6-bis[4-(5-hexyl-2,2'-bithiophene-5-yl)-phenyl]pyrrolo[3,4-c]-pyrrole-1,4-dione, 2,5-Diethylhexyl-3,6-bis[4-(5-hexyl-2,2'-bithiophene-5-yl)-phenyl]pyrrolo[3,4-c]-pyrrole-1,4-dione, and 2,5-Dihexyl-3,6-bis[4-(2,2'-bithiophene-5-yl)phenyl]pyrrolo[3,4-c]-pyrrole-1,4-dione. The chemical structures of the molecules are shown in Fig. 1. In the following, we label the four molecules as M1, M2, M3, and M4, respectively, for brevity. All molecules have similar chemical structures: compared to M2, M1 is two thiophene rings shorter; M3 has the side alkyl chains replaced by the ethyl-hexyl groups; M4 does not have the end alkyl chains. Therefore, comparisons among these molecules can reveal the dependence of exciton diffusion on conjugation length and the presence of alkyl chains. The crystalline structures of the molecules have been determined experimentally<sup>27</sup> where M3 was shown to have a different molecular packing from the others; the backbone of M3 molecule was distorted more severely than other molecules in the crystalline structure, which affects exciton diffusion as discussed

<sup>a)</sup>Electronic mail: ganglu@csun.edu

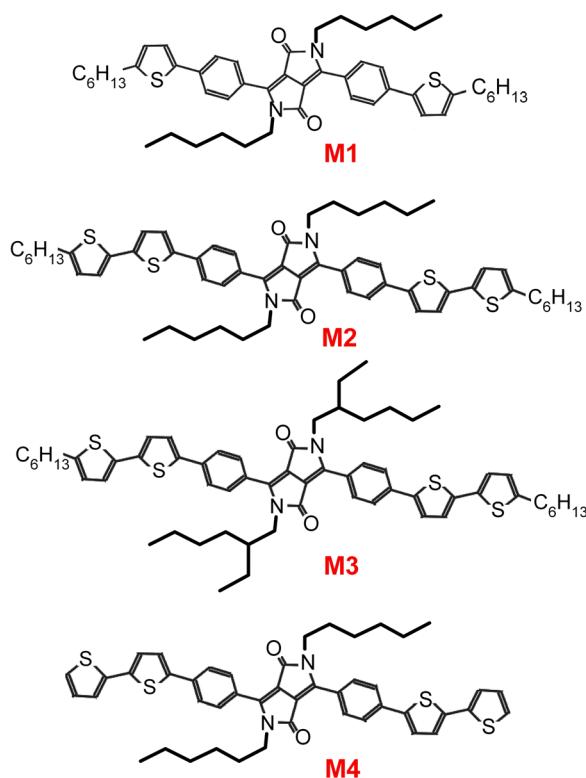


FIG. 1. Chemical structures of the four small conjugated molecules studied in this work.

below. Exciton diffusion properties in the four molecules have been examined experimentally<sup>10,14</sup> with  $L_D$  ranging from 4 to 13 nm in the order of  $M1 > M2 > M3 > M4$ .

The calculated  $L_D$ , exciton lifetime  $\tau$  and diffusivity  $D$  at 300 K in the disordered molecular structure are summarized in Table I. The standard deviations for  $L_D$  and  $\tau$  are obtained from 100 different molecular conformations for each molecule studied here. For each molecular conformation, 100 different exciton trajectories are sampled to determine a set of  $L_D$ ,  $\tau$ , and  $D$ . More computational details can be found in the supplementary materials. First of all, all computed quantities are in the same order of magnitude as the experimental results,<sup>10,14</sup> which is a preliminary validation of both the experimental and simulation results. Since the simulation results are obtained based on the disordered structures, this agreement with the experimental values suggests that exciton diffusion is primarily determined by the disordered domains in the materials, similar to the case in carrier mobilities.<sup>28</sup> In terms of  $L_D$ , we find  $M2 > M3$  and  $M2 > M4$ , which are consistent with the experimental trend.

TABLE I. Simulated exciton diffusion length  $L_D$  (nm), lifetime  $\tau$  (ns), and apparent diffusivity  $D$  ( $10^{-8}$  m<sup>2</sup>/s) in the disordered structure at 300 K. The standard deviations of the  $L_D$  and  $\tau$  are also listed. The last two rows show the intrinsic exciton diffusivity in 0.5 ns and 1.5 ns.

Symbol	M1	M2	M3	M4
$L_D$	$7.1 \pm 0.16$	$7.2 \pm 0.15$	$6.6 \pm 0.15$	$6.5 \pm 0.14$
$\tau$	$1.2 \pm 0.05$	$0.9 \pm 0.05$	$0.6 \pm 0.02$	$0.8 \pm 0.04$
$D$	4.1	5.5	7.5	5.5
$D$ (0.5 ns)	7.1	8.6	8.2	7.0
$D$ (1.5 ns)	4.0	4.5	4.4	4.2

However,  $L_D$  in M1 is similar to that in M2, which is at variance with the experimental result at the first sight. But as shown later, this discrepancy is resolved when the blend structure (the mixture of disordered and crystalline domains) is considered in the simulations.

$L_D$  is a function of exciton diffusivity and lifetime, and exciton diffusivity depends on exciton hopping rates between different excited states whereas exciton lifetime depends on exciton annihilation rates from the excited states to the ground state. From Table I, we see that the longer lifetime of M2 is mainly responsible for its larger diffusion length than M3 and M4, while the similar diffusion length of M1 and M2 is a result of M1's longer lifetime but smaller diffusivity as compared to M2.

In a disordered material, exciton annihilation is dominated by phonon-assisted as opposed to spontaneous recombination processes.<sup>15</sup> In addition, lower excitation energies usually lead to stronger couplings between the ground state and excited states, and thus shorter lifetimes as found in simulations.<sup>29,30</sup> The computed lowest excitation energies are listed in Table II and the trend in the excitation energies is consistent with the exciton lifetimes shown in Table I. These excitation energies are also close to the experimental values, ranging from 1.84 to 1.98 eV.<sup>27</sup> To correlate the excitation energies to the molecular structures, we find that the longer the backbone length, the more delocalized the conjugated  $\pi$  states, and thus the smaller the excitation energies. In M4, out of  $\sim 70\%$  of all molecular dynamics steps, the lowest exciton states exhibit a delocalized character; hence, the average excitation energy in M4 is lower than M2. This delocalization originates from a more compact packing of M4 thanks to the removal of the end alkyl chains. Also owing to the delocalized character, the exciton annihilation rates to the ground state are smaller in M4 than in M3. As a result, the lifetime of M4 is longer than M3 although their excitation energies are very close.

Similar to carrier transport,<sup>31</sup> exciton diffusivity relates to exciton lifetime—the longer the lifetime, the higher the probability that the exciton may encounter traps, and hence the lower the apparent diffusivity. Note that traps here are not recombination centers, thus excitons can still escape from the traps. We do not consider the recombination centers in this paper, although they have been observed experimentally.<sup>32</sup> To provide a better estimate of their intrinsic diffusivity, we calculate the diffusivity of the molecules in the *same* time interval of 0.5 ns and 1.5 ns. In other words, we try to disentangle the diffusivity from the lifetime. For both cases, we find that M2 has the highest intrinsic diffusivity, suggesting that exciton transport in M2 is the easiest among the four molecules. Overall, this intrinsic diffusivity

TABLE II. Averaged lowest excitation energy  $\bar{E}$  (eV) during the molecular dynamics simulations, its standard deviation  $\Delta E$  (eV), and averaged atomic displacement  $\delta d$  (Å).

Symbol	M1	M2	M3	M4
$\bar{E}$	2.0	1.8	1.6	1.6
$\Delta E$	0.106	0.088	0.094	0.073
$\delta d$	0.92	0.93	1.40	0.70

correlates well to the apparent diffusivity. However, M3 displays a lower intrinsic diffusivity but a higher apparent diffusivity than M2, indicating that its higher apparent diffusivity is mainly due to its shorter lifetime. This result is in line with the experimental findings<sup>14</sup> that the diffusivity of M3 could be either higher or lower than that of M2, depending on the experimental techniques for the measurement; the different techniques yielded different lifetimes for both M2 and M3, thus different apparent diffusivities. Exciton intrinsic diffusivity is determined by exciton hopping rates, which in turn hinge on the energetic disorder of the material. The energetic disorder is a measure of exciton hopping energy barriers and can be defined as the standard deviation of the lowest exciton energies during the molecular dynamics (MD) simulations. The values of the energetic disorder are listed in Table II. We find that M2 exhibits a lower energetic disorder than M1 and M3, which explains its higher intrinsic diffusivity. Although M4 has the lowest energetic disorder, it also has a rather low apparent exciton diffusivity; this may be due to the existence of low-energy intermolecular excitons (intermolecular excitons tend to have lower mobilities than intramolecular excitons).

We could further correlate the energetic disorder with the structural rigidity of the molecules. The structural rigidity can be characterized by molecular deformations during the MD simulations. More specifically, here we take the average atomic displacements from the backbone plane as an indicator for its structural rigidity. Table II lists the average atomic displacement  $\delta d$  for the molecules. Although M2, M3, and M4 share the same backbone structure, their structural rigidity is different, in the order of  $M4 > M2 > M3$  ( $M4$  being more rigid than  $M2$  and  $M3$ ); this trend of molecular rigidity is consistent with the trend of energetic disorder. The lower structural rigidity of  $M3$  is confirmed by the experiment where the crystalline structure of  $M3$  showed a higher degree of deformation.<sup>27</sup>  $M4$  is the most rigid molecule thanks to the removal of flexible end alkyl chains. Because  $M1$  and  $M2$  have different backbone structures, it is more appropriate to compare the atomic displacement of  $M2$  to  $M1$  without including the two ending thiophene rings. In this case, the atomic displacement of  $M2$  is  $0.79 \text{ \AA}$ , smaller than that of  $M1$ , leading to a lower energetic disorder.

In the following, we discuss the anisotropy of exciton diffusion in the crystalline structure with  $M2$  as an example. Since  $M1$  and  $M2$  have the similar crystalline structure, they share the similar exciton diffusion anisotropy. The molecular packing of the crystalline  $M2$  is displayed in Fig. 2(a) with the unit cell represented by the dashed box. Each solid line denotes a molecule ( $M1$  or  $M2$ ) whose backbone is along  $z$  direction. Note that Fig. 2(a) is only a schematic rendition of the real crystalline structure in which the unit cell is monoclinic and each molecule is tilted relative to the  $z$  axis. Here, we focus on exciton diffusion along two directions, T1 and T2. The T1 direction connects the center of the two molecules in the same unit cell, whereas T2 connects the two molecules from neighboring unit cells, along the  $\pi$ - $\pi$  stacking direction. Our Monte Carlo simulations indicate that in both  $M1$  and  $M2$ ,  $\sim 75\%$  exciton hops are along T1 direction while only a small portion ( $\sim 5\%$ ) along T2. The contributions from the other directions amount to the remaining

$\sim 20\%$ . We discover that the exciton diffusion takes place primarily on the plane of YOZ, as shown in Fig. S1 of supplementary material.<sup>26</sup> In the interest of space, the detailed results of exciton diffusion anisotropy are shown in the supplementary material. The diffusion anisotropy between T1 and T2 is a result of different exciton transition rates along the two directions. Although the intermolecular distances in T1 and T2 are similar, the exciton transition rates in T1 direction are one order of magnitude higher than those in T2 direction. The exciton transition rate is proportional to the square of the Coulomb interaction between two transition densities, one at each molecule. The Coulomb interaction in turn depends on the spatial distribution of the transition density in each molecule and the relative position between the two molecules.<sup>23</sup> In Fig. 2(b), we display the transition density distribution in  $M2$ , with the positive (negative) density on the lower (upper) half of the molecule, yielding a transition dipole along the backbone (the pink arrow). In Fig. 2(c), we illustrate that the Coulomb interaction between the transition densities along T1 direction is much stronger than that along T2 direction. Here, the solid horizontal line denotes the molecule backbone along  $z$  axis, and  $+$  ( $-$ ) sign indicates the positive (negative) transition density. In T1 direction, the relative shift between the neighboring backbones is small ( $\sim 4 \text{ \AA}$ ), hence the Coulomb energy is dominated by the interaction between the like charges in the oval circles. In contrast, the backbone shift in T2 direction is larger ( $\sim 9 \text{ \AA}$ ), and as a result the Coulomb interaction between the like charges

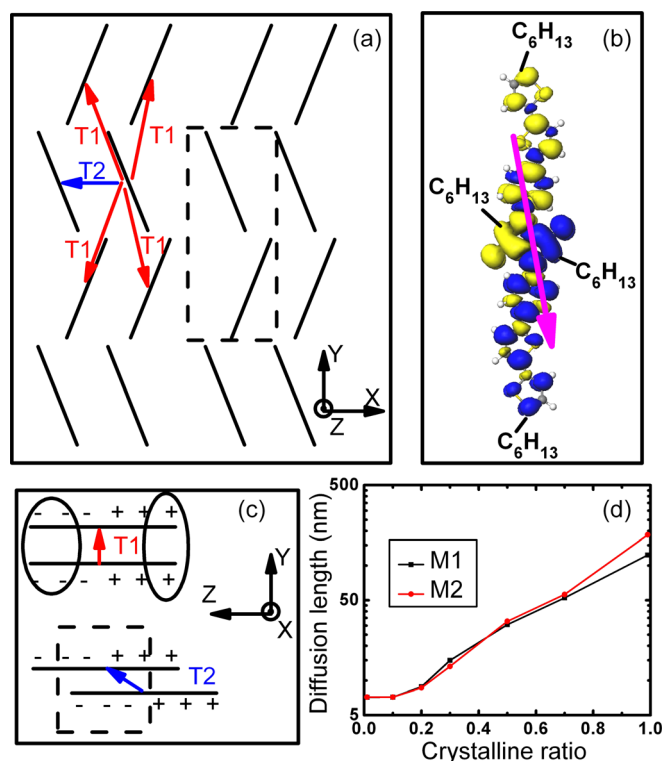


FIG. 2. (a) Schematic crystalline structure of  $M2$  and the dashed box indicates the unit cell. (b) The transition density for the lowest exciton state in  $M2$ ; the blue (yellow) isosurface represents the charge density distribution at  $+(-) 0.01 \text{ \AA}^3$  and the pink arrow denotes the direction of the transition dipole. (c) Illustration of different backbone shifts in T1 and T2 directions; the symbol “+” (“-”) indicates a positive (negative) transition density along the backbone. (d) Exciton diffusion length as a function of the crystalline ratio in the blend structures of  $M1$  and  $M2$ .



is partially canceled by that between the opposite charges as shown schematically in the dashed box. Therefore, the net Coulomb interaction in T1 direction is stronger than that in T2 direction, explaining the exciton transition rate differences in the two directions.

To understand the discrepancy between the simulation and the experiment with regard to  $L_D$  in M1 and M2, we consider exciton diffusion in a blend structure which consists of a mixture of disordered and crystalline domains. Fig. 2(d) shows  $L_D$  as a function of crystalline ratio  $\alpha$  for the blend structure. As  $\alpha$  increases from 0 to 1, i.e., from a complete amorphous system to a crystalline,  $L_D$  increases by one order of magnitude. Furthermore,  $L_D$  changes very slowly below  $\alpha = 0.2$ , and then rises rapidly as  $\alpha \geq 0.3$ . The sharp raise is probably due to the formation of percolated crystalline domains in the blend. We find that  $L_D$  in M1 is similar to M2 at low crystalline ratios, but lower than M2 at high ratios. However, if the crystalline ratio in M1 is higher in M2, it is possible that  $L_D$  in M1 is actually larger than M2, which then reconciles the discrepancy between the simulation and the experiment. This speculation is indeed true—the experiment has shown that the crystallinity of M1 is higher than M2.<sup>14</sup> Therefore, by considering exciton diffusion in a blend structure, we can reproduce the experimental trend in  $L_D$  for all four molecules. Moreover, based on the results in Fig. 2, we predict that the crystalline ratio of M1 is about 30%. Since  $L_D$  of the three molecules (M2-M4) measured in the experiment is similar to what was computed in the disordered domain, we infer that their crystalline ratio should be less than 20%. Although there is no precise experimental measurement on the crystalline ratio, the experimental results indeed suggested a relative low crystallinity in the three molecules, consistent with our analysis.

To summarize, first-principles simulations are carried out to study exciton diffusion in a series of small conjugated molecules in disordered crystalline and blend structures. An overall good agreement between the experiment and simulations is achieved. The correlation between exciton diffusion and molecular structure is examined in detail. In the disordered structure, we find that a longer backbone length leads to a shorter exciton lifetime and a higher exciton diffusivity, but it does not change  $L_D$  substantially. The removal of the end alkyl chains or the extra branch on the side alkyl chains is found to reduce  $L_D$ . In the crystalline structure, exciton diffusion exhibits a strong anisotropy resulting from directional transition density interactions. In the blend structure,  $L_D$  increases with the crystalline ratio; we predict M1 has a higher crystallinity than the other three molecules. The crystalline ratio is estimated to be about 30% in M1 and should be less than 20% in other three molecules. Our simulations suggest that a longer molecular backbone is beneficial to exciton diffusion provided the crystallinity is preserved. Although the modification of the side and end chains may enhance exciton diffusion by yielding favorable molecular packing, it should be carried out with minimal distortions of the backbone. Finally, one should minimize the relative shift between neighboring backbones in designing the crystal structure of the conjugated small molecules.

We thank Thuc-Quyen Nguyen, Jason Lin, and Oleksandr V. Mikhnenko for critical reading of the manuscript and valuable discussions. The work was supported by the NSF Solar Grant (No. DMR-1035480), NSF PREM Grant (No. DMR-1205734), and the Office of Naval Research.

- <sup>1</sup>A. Mayer, S. Scully, B. Hardin, M. Rowell, and M. McGehee, *Mater. Today* **10**, 28 (2007).
- <sup>2</sup>J. J. M. Halls, K. Pichler, R. H. Friend, S. C. Moratti, and A. B. Holmes, *Appl. Phys. Lett.* **68**, 3120 (1996).
- <sup>3</sup>C. L. Yang, Z. K. Tang, W. K. Ge, J. N. Wang, Z. L. Zhang, and X. Y. Jian, *Appl. Phys. Lett.* **83**, 1737 (2003).
- <sup>4</sup>D. E. Markov, E. Amsterdam, P. W. M. Blom, A. B. Sieval, and J. C. Hummelen, *J. Phys. Chem. A* **109**, 5266 (2005).
- <sup>5</sup>S. R. Scully and M. D. McGehee, *J. Appl. Phys.* **100**, 034907 (2006).
- <sup>6</sup>S.-B. Rim, R. F. Fink, J. C. Schoneboom, P. Erk, and P. Peumans, *Appl. Phys. Lett.* **91**, 173504 (2007).
- <sup>7</sup>P. E. Shaw, A. Ruseckas, and I. D. W. Samuel, *Adv. Mater.* **20**, 3516 (2008).
- <sup>8</sup>R. R. Lunt, N. C. Giebink, A. A. Belak, J. B. Benziger, and S. R. Forrest, *J. Appl. Phys.* **105**, 053711 (2009).
- <sup>9</sup>M. C. Fravventura, J. Hwang, J. W. A. Suijkerbuijk, P. Erk, L. D. A. Siebbeles, and T. J. Savenije, *J. Phys. Chem. Lett.* **3**, 2367 (2012).
- <sup>10</sup>O. V. Mikhnenko, J. Lin, Y. Shu, J. E. Anthony, P. W. M. Blom, T.-Q. Nguyen, and M. A. Loi, *Phys. Chem. Chem. Phys.* **14**, 14196 (2012).
- <sup>11</sup>J. E. Kroeze, T. J. Savenije, M. J. W. Vermeulen, and J. M. Warman, *J. Phys. Chem. B* **107**, 7696 (2003).
- <sup>12</sup>L. Luer, H. J. Egelhaaf, D. Oelkrug, G. Cerullo, G. Lanzani, B. H. Huisman, and D. de Leeuw, *Org. Electron.* **5**, 83 (2004).
- <sup>13</sup>S. Cook, H. Liyuan, A. Furube, and R. Katoh, *J. Phys. Chem. C* **114**, 10962 (2010).
- <sup>14</sup>J. D. A. Lin, O. V. Mikhnenko, J. Chen, Z. Masri, A. Ruseckas, A. Mikhailovsky, R. P. Raab, J. Liu, P. W. M. Blom, M. A. Loi, C. J. Garcia-Cervera, I. D. W. Samuel, and T.-Q. Nguyen, *Mater. Horiz.* **1**, 280–285 (2014).
- <sup>15</sup>X. Zhang, Z. Li, and G. Lu, *Phys. Rev. B* **84**, 235208 (2011).
- <sup>16</sup>H. Iikura, T. Tsuneda, T. Yanai, and K. Hirao, *J. Chem. Phys.* **115**, 3540 (2001).
- <sup>17</sup>T. Stein, H. Eisenberg, L. Kronik, and R. Baer, *Phys. Rev. Lett.* **105**, 266802 (2010).
- <sup>18</sup>A. Karolewski, T. Stein, R. Baer, and S. Kummel, *J. Chem. Phys.* **134**, 151101 (2011).
- <sup>19</sup>W. R. Duncan, W. M. Stier, and O. V. Prezhdo, *J. Am. Chem. Soc.* **127**, 7941 (2005).
- <sup>20</sup>S. G. Abuabara, L. G. C. Rego, and V. S. Batista, *J. Am. Chem. Soc.* **127**, 18234 (2005).
- <sup>21</sup>W. Mou, S. Hattori, P. Rajak, F. Shimojo, and A. Nakano, *Appl. Phys. Lett.* **102**, 173301 (2013).
- <sup>22</sup>S. C. J. Meskers, J. Hubner, M. Oestreich, and H. Bassler, *J. Phys. Chem. B* **105**, 9139 (2001).
- <sup>23</sup>E. Hennebicq, G. Pourtois, G. D. Scholes, L. M. Herz, D. M. Russell, C. Silva, S. Setayesh, A. C. Grimsdale, K. Mullen, J. L. Brédas, and D. Beljonne, *J. Am. Chem. Soc.* **127**, 4744 (2005).
- <sup>24</sup>C. Madigan and V. Bulovic, *Phys. Rev. Lett.* **96**, 046404 (2006).
- <sup>25</sup>M. E. Köse, P. Graf, N. Kopidakis, S. E. Shaheen, K. Kim, and G. Rumbles, *ChemPhysChem* **10**, 3285 (2009).
- <sup>26</sup>See supplementary material at <http://dx.doi.org/10.1063/1.4871303> for simulation details and the results of anisotropy of exciton diffusion in crystalline domain.
- <sup>27</sup>C. Kim, J. Liu, J. Lin, A. B. Tamayo, B. Walker, G. Wu, and T.-Q. Nguyen, *Chem. Mater.* **24**, 1699 (2012).
- <sup>28</sup>R. A. Street, J. E. Northrup, and A. Salleo, *Phys. Rev. B* **71**, 165202 (2005).
- <sup>29</sup>J. M. An, M. Califano, A. Franceschetti, and A. Zunger, *J. Chem. Phys.* **128**, 164720 (2008).
- <sup>30</sup>W. Mou, S. Ohmura, F. Shimojo, and A. Nakano, *Appl. Phys. Lett.* **100**, 203306 (2012).
- <sup>31</sup>N. Vukmirović, C. S. Ponseca, H. Némec, A. Yartsev, and V. Sundström, *J. Phys. Chem. C* **116**, 19665 (2012).
- <sup>32</sup>O. V. Mikhnenko, M. Kuik, J. Lin, N. van der Kaap, T.-Q. Nguyen, and P. W. M. Blom, *Adv. Mater.* **26**, 1912 (2014).